J. Fluid Mech. (1991), *vol.* 222, *pp.* 437–447
Printed in Great Britain

Experiments on vortex shedding from flat plates with square leading and trailing edges

By YASUHARU NAKAMURA, YUJI OHYA AND HIDEKI TSURUTA

Research Institute for Applied Mechanics, Kyushu University, Kasuga 816, Japan

(Received 26 September 1989)

Vortex shedding from flat plates with square leading and trailing edges having chord-to-thickness ratios 3–16 at Reynolds numbers $(1–3)\times10^3$ is investigated experimentally in low-speed wind tunnels. It is shown that vortex shedding from flat plates with square leading and trailing edges is characterized by the impinging-shear-layer instability where the separated shear layer becomes unstable in the presence of a sharp trailing edge corner. The Strouhal number which is based on the plate's chord is approximately constant and equal to 0.6 for chord-to-thickness ratios 3–5. With further increase in the ratio it increases stepwise to values that are approximately equal to integral multiples of 0.6.

1. Introduction

Vortex shedding from elongated bluff cylinders has received increasing attention since it is associated with many cases of flow-induced structural and acoustic vibrations. Vortex shedding from short bluff cylinders including circular and square-section ones has been studied in many papers. By contrast, only a few papers have been published on vortex shedding from elongated bluff cylinders. These include Okajima, Mizota & Tanida (1983), Parker & Welsh (1983), Stokes & Welsh (1986) and Nakamura & Nakashima (1986).

In their paper Stokes & Welsh (1986) summarized the results obtained by Parker & Welsh (1983) on flat plates with square leading and trailing edges for various values of the chord-to-thickness ratio c/t, where c is chord and t is thickness. The range of the Reynolds number in their experiment, which was based on the thickness t, was $Re = (1.5–3.1)\times10^4$ approximately.

According to Stokes & Welsh, there are four possible vortex shedding regimes depending on c/t.

(a) On short plates ($c/t < 3.2$) flow separation occurs at the leading-edge corners and the shear layers interact directly, without reattaching to the plate's surface, to form a regular vortex street.

(b) On longer plates ($3.2 < c/t < 7.6$) the shear layers reattach to the trailing-edge surface periodically in time and form a regular vortex street in the wake.

(c) For still longer plates ($7.6 < c/t < 16$) the shear layers are always reattached upstream of the trailing edges and form a separation bubble which grows and divides in a random manner. The vortices are distributed randomly throughout the boundary layers and consequently produce irregular shedding and no clear regular vortex street.

(d) For plates with $c/t > 16$ the separation bubbles fluctuate in length in the same manner as described in (c) but the randomly distributed vortices diffuse before

reaching the trailing edge. Behind the plate, the fully developed turbulent shear layers form a regular vortex street not directly related to the formation of the leading-edge separation bubbles.

Okajima *et al.* (1983) also identified regimes (*a*)–(*c*) on the basis of measurements on flat plates with $c/t = 1$–9.

In our previous paper (Nakamura & Nakashima 1986) on bluff cylinders with elongated rectangular, H and ⊢ cross-sections, made independently of the work of Parker & Welsh (1983), we arrived at a somewhat different interpretation about vortex shedding in regime (*b*). Namely, the flow in regime (*b*) is characterized by the impinging-shear-layer instability (Rockwell & Naudascher 1978), where the separated shear layer becomes unstable in the presence of a sharp trailing-edge corner. We showed that the shear layers of an elongated bluff cylinder can be unstable even when a splitter plate is placed behind it. When the splitter is removed, the two unstable shear layers, the upper and lower ones, interact with each other, and, by adjusting the phase of shedding with the frequency unchanged, form a regular vortex street. The Strouhal number for various values of c/t, based on the chord c, was found to be approximately constant and equal to 0.6, irrespective of the cross-section geometry.

In our previous experiment, however, the tested range of c/t for rectangular cylinders (i.e. flat plates, as referred to in this paper) was limited covering only from 2 to 5.5. Therefore, it is worth asking, in the light of our findings, what happens in regimes (*c*) and (*d*) when increasing the value of c/t beyond 5.5. The present paper is concerned with measurements on vortex shedding from flat plates with square leading and trailing edges with c/t ranging from 3 to 16 at Reynolds numbers $(1$–$3) \times 10^3$.

Incidentally, the description concerning regime (*a*) for short plates, made by Stokes & Welsh, needs some correction. The two separated shear layers do not always interact directly. At c/t below a critical value, close to 0.6, they are free to interact, while they are not free at c/t beyond the critical. At c/t beyond the critical, the shear-layer/edge direct interaction (see Nakamura & Hirata 1989, for example) can occur so that the critical c/t is characterized by a marked increase in mean drag and mean base suction. However, this phenomenon is outside the scope of the present investigation.

2. Experimental arrangements

The experiment consisted of measurements of vortex-shedding frequency using hot-wire anemometers and flow visualization using smoke. The measurement of vortex-shedding frequency was made in a wind tunnel with a rectangular working section 3 m high, 0.7 m wide and 2 m long. The turbulence intensity of the free stream was less than about 0.3%. As is shown in figure 1, the models used in the experiment were flat plates with square leading and trailing edges that were made of aluminium. The thickness t of each plate was constant and equal to 6 mm while the chord c was widely varied, and the resulting chord-to-thickness ratio c/t ranged from 3 to 16. Each model had 200 mm × 500 mm end plates with a separation of 600 mm (figure 1), and was mounted horizontally at zero incidence across the centre of the working section. The resulting span-to-chord ratio ranged from 6.7 to 33.3, which was large enough to maintain two-dimensional flow conditions.

In the experiment, the velocity fluctuation was detected using hot-wire anemometers, and four positions of I-type probes, three above the plate and one in

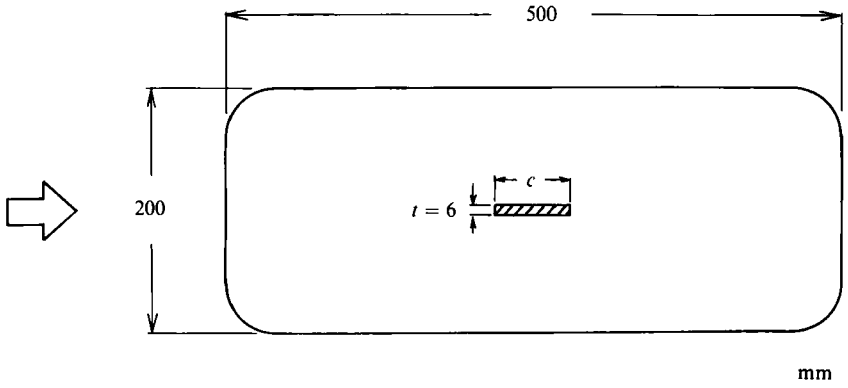

FIGURE 1. A flat-plate model with end plates.

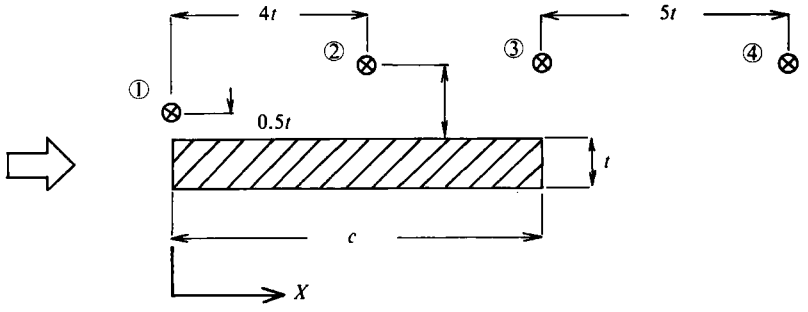

FIGURE 2. Positions of hot-wire probes used in the experiment. X is the streamwise distance measured from the leading edge.

the wake, were chosen, as shown in figure 2. The flow velocity was varied over a range of $U = 2.5$–7.5 ms^{-1} approximately, where U is the velocity of the free stream, so that the range of the Reynolds number, based on the thickness, was $Re = (1\text{–}3) \times 10^3$.

The vortex-shedding frequency was determined using a FFT wave analyser, and the Strouhal number $S(c) = f_v c/U$ was obtained, where f_v is the dominant shedding frequency. Since the model was very small relative to the tunnel working section, no blockage corrections have been applied to the results of the present measurement.

When a dominant shedding frequency was detected, the variation of the phase of vortex shedding along the plate's surface was measured. Two I-type probes were used for this purpose. One probe was fixed as a reference at either the leading edge (1 in figure 2) or the trailing edge (3 in figure 2) while the other was traversed along the plate's surface, and the phase angle of the velocity fluctuation was determined using the FFT wave analyser. When more than one dominant frequency was found, the phase measurement was made at each of the dominant frequencies.

Flow visualization using liquid paraffin smoke was made in a wind tunnel with a rectangular working section 2 m high, 4 m wide and 6 m long. The turbulence intensity of the free stream was about 0.12 %. The test was made on a flat plate with $c/t = 8$. Three wooden models with different values of t, i.e. 15, 30 and 40 mm, were used. Each model had 1 m × 1.25 m transparent end plates with a separation of 1.88 m, and was mounted at zero incidence across the centre of the working section. The flow velocity was varied over a range of $U = 0.33$–1.0 ms^{-1} approximately to obtain the same Reynolds number range $Re = (1\text{–}3) \times 10^3$ as in the Strouhal-number measurements.

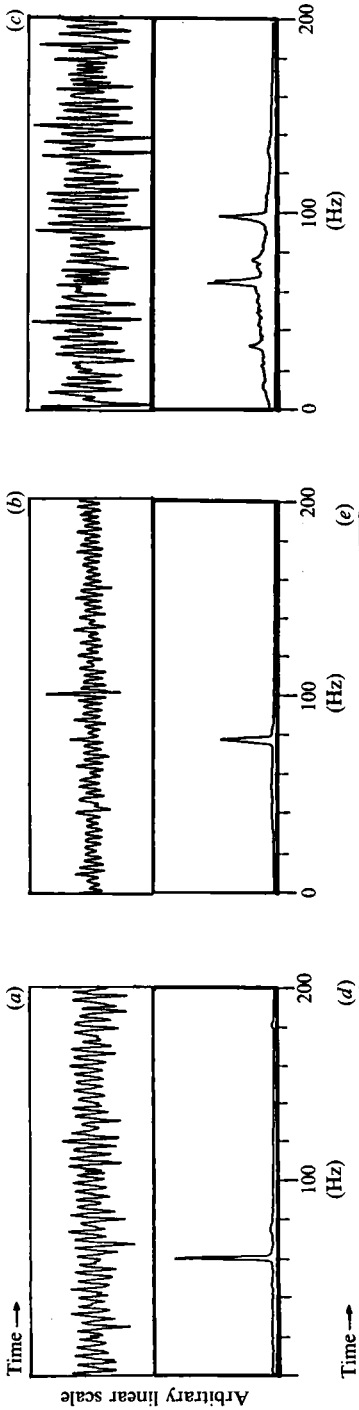

FIGURE 3. Velocity fluctuations and power spectra (linear scale) for various values of chord-to-thickness ratio. (*a*) $c/t = 4$; (*b*) 6; (*c*) 8; (*d*) 10; (*e*) 14.

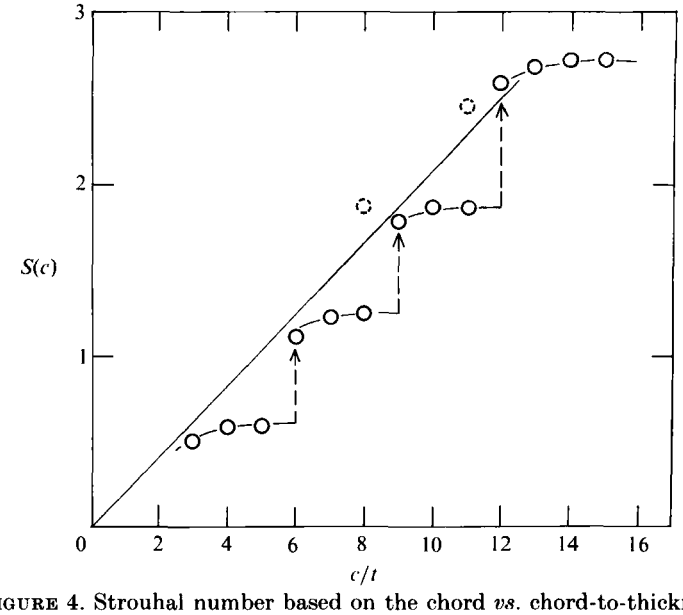

FIGURE 4. Strouhal number based on the chord *vs.* chord-to-thickness ratio.

3. Experimental results and discussions

3.1. *Power spectra of velocity fluctuation, Strouhal number and phase angle of vortex shedding*

Figure 3 shows some selected time histories and power spectra of the velocity fluctuation for flat plates with various values of c/t at $Re = 10^3$. Remember that the measurement was made with constant t and U. The signals were taken from the probes at the trailing edge and in the wake (figure 2). In general the velocity fluctuations were weakest at the leading edge but they became strong enough at the trailing edge and in the wake to detect the spectral peak.

Most spectra had one dominant frequency peak while some had two such peaks (e.g. figure 3*c*). Dominant peaks in the spectra were detected for c/t up to 15. At $c/t = 16$ the spectra were broadbanded with no dominant peaks. The general trend observed is that the value of the dominant frequency was gradually decreased with increasing c/t and then jumped to a higher value at a certain value of c/t. Decrease and jump in frequency repeated with increasing c/t. Two dominant frequencies appeared at the jump. However, this does not mean that the signal contained two dominant-frequency components simultaneously. On the contrary, it had normally only one dominant frequency, and time intervals with a different dominant frequency repeated at random one after another.

Figure 4 shows the variation of the Strouhal number $S(c)$ with the chord-to-thickness ratio. $S(c)$ is nearly constant and equal to 0.6 for $c/t = 3$–5, which is in good agreement with our previous measurements (Nakamura & Nakashima 1986). However, what is new and interesting in this investigation is that with further increase in c/t, $S(c)$ increases stepwise to values that are approximately equal to integral multiples of 0.6. Accordingly, each branch of nearly constant $S(c)$ is given an integer n. $S(c)$ has often two values at the jump. Full circles correspond to the higher peaks in the spectra while broken circles correspond to the lower ones. The points at which each branch starts are on a straight line passing the origin.

In figure 5 the phase angle of the velocity fluctuation at the dominant frequency,

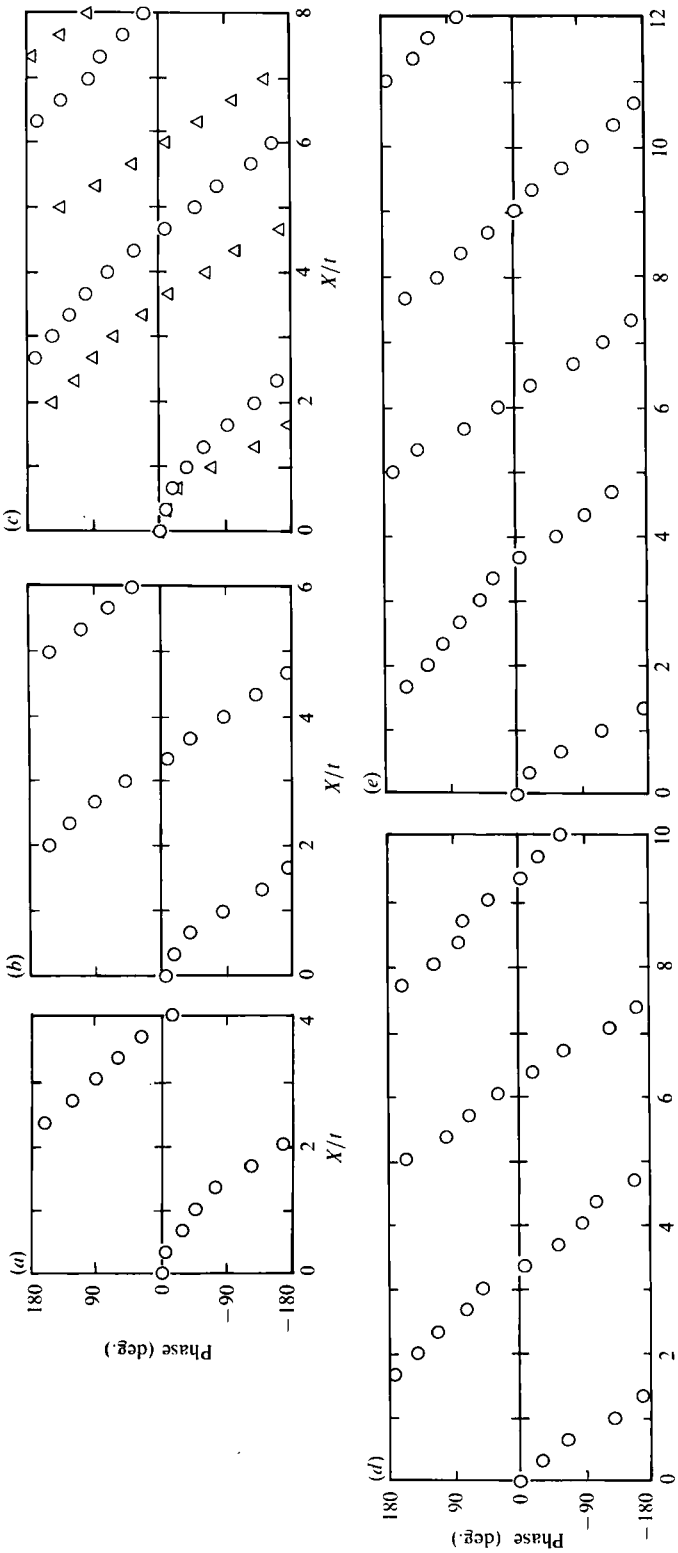

FIGURE 5. Phase angle of vortex shedding measured on the side face. (*a*) $c/t = 4$; (*b*) 6; (*c*) 8; ○, $n = 2$; △, $n = 3$; (*d*) 10; (*e*) 12.

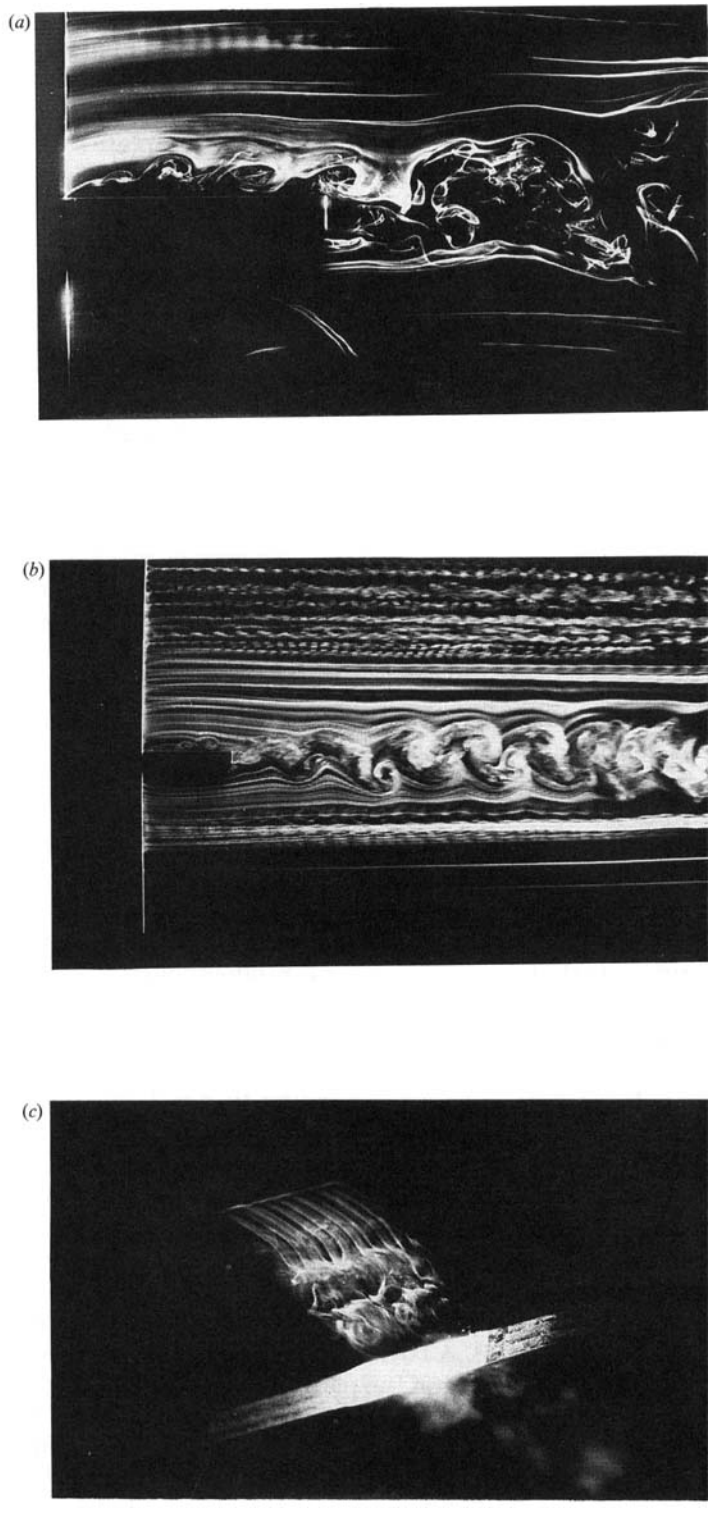

FIGURE 6. Visualization of the flow past a flat plate with $c/t = 8$ at $Re = 10^3$. (*a*) Side view, $n = 3$; (*b*) side view, $n = 2$; (*c*) slantwise view, $n = 2$.

measured relative to that at the leading edge, is plotted against the distance along the chord for various values of c/t. As can be seen, there is a simple relation between the wavelength of the velocity fluctuation and the plate's chord. That is, in accordance with the results shown in figure 4, the wavelength is just equal ($n = 1$ and 2) or approximately equal ($n = 3$ and 4) to fractions of the plate's chord. In other words, the integer n represents the number of vortices that are formed on the plate's surface. Figure 5(*c*) again indicates that a flat plate with $c/t = 8$ is characterized by vortex shedding with $n = 2$ and 3.

3.2. *Impinging-shear-layer instability*

It has now become clear that vortex shedding from flat plates with square leading and trailing edges having c/t up to 15 is characterized by the impinging-shear-layer instability. According to Rockwell & Naudascher (1978), the shear-layer instability is greatly enhanced by the feedback control of the impinging edge on the vorticity production at the separation point. It thus appears that the discontinuity of the boundary condition imposed at the trailing edge is essential to enhance the shear-layer instability. It should be added that the impinging edge does not need to be sharp to trigger the instability, although a sharp one may be ideal. In fact, Stokes & Welsh (1986) found that substituting semi-circular for square trailing edges made little difference to the vortex shedding. As will be discussed in §3.5, even a flat surface can trigger the instability.

The impinging-shear-layer instability initiates at about $c/t = 3$ where the wavelength of vortex shedding is just equal to the plate's chord. As c/t is increased, the wavelength is locked-on to the plate's chord through some nonlinear flow processes until a certain limit is reached. At the limit, transition of the mode of vortex shedding from $n = 1$ to $n = 2$ occurs, as has been depicted in the preceding section. With a further increase in c/t the same cycle of events repeats.

3.3. *Flow visualization*

The experiment using smoke indicated that the flow around a flat plate with $c/t = 8$ at around $Re = 10^3$ is turbulent with inherent random fluctuations. Figure 6(*a*) presents a close-up side view of the flow pattern at $Re = 10^3$. It shows a short-wave instability on the shear layer occurring about $1t$ downstream of the separation point which is followed by a long-wave instability. The long-wave instability seems to be the impinging-shear-layer instability corresponding to $n = 3$, while the short-wave one could be the shear-layer instability not directly related to the flow impingement. The mode of vortex shedding $n = 3$ was determined by the simultaneous hot-wire measurement of the Strouhal number. The onset of the short-wave instability marks the transition of the shear layer from laminar to turbulent. Tomonari (1988) also observed, in his measurements on low-Re galloping of a square-section cylinder, that the transition point on the shear layer was close to the trailing-edge corner of the cylinder at Reynolds numbers around 10^3. Figure 6(*b*) shows the vortex shedding corresponding to $n = 2$ at $Re = 10^3$. A fairly regular vortex street is seen in the wake but no detail is known about the flow on the plate's surface. Figure 6(*c*) is a slantwise view of the separated flow on the same plate, where it is seen that the flow after separation is initially two-dimensional but three-dimensional random modulations are developed when the curvature of the shear layer is reversed. Such three-dimensional modulations are common in many complex turbulent flows (Taneda 1983).

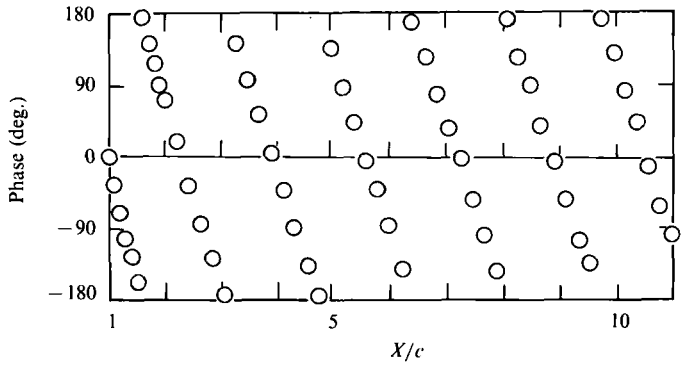

FIGURE 7. Phase angle of vortex shedding measured in the wake for a flat plate with $c/t = 4$.

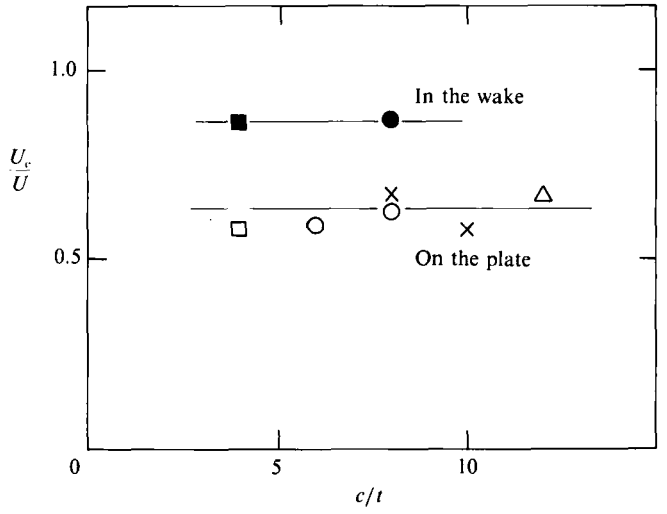

FIGURE 8. Phase velocity of vortex shedding measured on the side face and in the wake. □, ■, $n = 1$; ○, ●, $n = 2$; ×, $n = 3$; △, $n = 4$.

3.4. *Vortex-shedding characteristics in the wake*

The smoke-flow patterns shown in figure 6(*b*) suggest an interesting feature that the wavelength of vortex shedding in the wake may be much larger than that on the side face of a plate. In order to verify this, we added a measurement of the vortex-shedding phases in the wake on flat plates with $c/t = 4$ and 8.

Figure 7 shows the phase angle of the velocity fluctuation for a flat plate with $c/t = 4$, plotted against the distance along the wake. As can be seen, the wavelength of vortex shedding in the wake over a range of $X/c = 2$–10 is nearly constant and equal to $1.7c$, which is much larger than the wavelength of $1c$, measured on the side face (figure 5*a*). The results for a flat plate with $c/t = 8$, not shown here, were similar to those shown in figure 7.

We can compute the phase velocity U_c of vortex shedding using measured frequency and wavelength. Figure 8 shows the results for U_c/U, the phase velocity of vortex shedding relative to the free-stream velocity plotted against c/t. It is interesting that the value of U_c/U on the side face is approximately constant and equal to 0.63 while U_c/U in the wake is approximately equal to 0.86. The phase

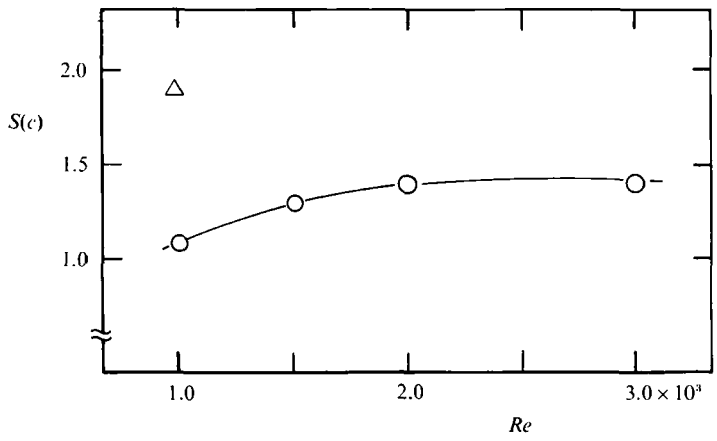

FIGURE 9. Variation of the Strouhal number with the Reynolds number for a flat plate with $c/t = 8$. ○, $n = 2$; △, $n = 3$.

velocity of vortex shedding may be approximated by the mean velocity across the shear layer. The velocity defect inside the separation bubble is considerable so that the mean velocity across the shear layer is small. On the other hand, the velocity defect in the wake should be reduced so that the mean velocity across the shear layer increases.

3.5. *Effects of the Reynolds number on vortex shedding*

Figure 9 shows a plot of the Strouhal number against the Reynolds number for a flat plate with $c/t = 8$. With increasing Re the Strouhal number increases gradually and appears to asymptote a constant value at higher Re.

The general trend observed in the velocity fluctuations is that as the Reynolds number was increased, dominant peaks in the spectra became less sharp. For $c/t > 12$ at $Re > 2 \times 10^3$ the spectra were broadbanded with no dominant peaks. Nevertheless, this does not mean that the impinging-shear-layer instability vanishes at high Reynolds numbers. In fact, Stokes & Welsh (1986) were able to show in their experiments on flat plates at $Re = (8\text{–}44.3) \times 10^3$ that although natural shedding was not detectable, resonant peaks due to applied sound appeared at around the Strouhal numbers corresponding to $n = 1$–4 shown in the present figure 4. That is, although the impinging-shear-layer instability at high Reynolds numbers may be masked by inherent turbulent fluctuations and may often be difficult to detect, it does not vanish and can be excited by external forcings. This is characteristic of the flow instability in general. For example, coherent structures in turbulent boundary layers were also detected by external forcings (Taneda 1981).

For the reason mentioned above, vortex shedding with $n \geqslant 5$ may well be formed on flat plates with $c/t \geqslant 16$. Recent observations by Cherry, Hillier & Latour (1983, 1984) showed that the separated-and-reattaching flow is not always steady but has vortex shedding of weak periodicity. The Strouhal number has a value of roughly 0.7 if it is based on the mean reattachment length (Cherry *et al.* 1983). As mentioned earlier (Nakamura & Nakashima 1986), the impinging-shear-layer instability is responsible for the weak vortex shedding of the separated-and-reattaching flow. Thus, the Strouhal number for the separated-and-reattaching flow past a very long flat plate may vary along the straight line shown in figure 4, if it is based on the plate's chord.

4. Conclusions

The wind-tunnel experiments showed that vortex shedding from flat plates with square leading and trailing edges having chord-to-thickness ratios $c/t = 3$–15 at Reynolds numbers $(1\text{–}3)\times10^3$ was characterized by the impinging-shear-layer instability where the separated shear layer becomes unstable in the presence of a sharp trailing-edge corner. The Strouhal number which was based on the plate's chord was approximately constant and equal to 0.6 for $c/t = 3$–5. With a further increase in c/t up to 15 it increased stepwise to values that were approximately equal to integral multiples of 0.6.

For flat plates with $c/t > 12$ and at $Re > 2\times10^3$, spectra of the velocity fluctuations were broadbanded with no dominant peaks. However, this does not mean that the impinging-shear-layer instability vanishes at high Reynolds numbers. It can be excited by external forcings, as Stokes & Welsh (1986) showed in their experiments on the effects of applied sound on vortex shedding.

We thank Messrs N. Fukamachi, K. Watanabe and A. Kawahara for technical assistance in conducting the experiment. The manuscript was typed by Mrs Y. Iwaki.

REFERENCES

CHERRY, N. J., HILLIER, R. & LATOUR, M. E. M. P. 1983 The unsteady structure of two-dimensional separated and reattaching flows. *J. Wind Engng Indust. Aero.* **11**, 95–105.

CHERRY, N. J., HILLIER, R. & LATOUR, M. E. M. P. 1984 Unsteady measurements in a separated and reattaching flow. *J. Fluid Mech.* **144**, 13–46.

NAKAMURA, Y. & HIRATA, K. 1989 Critical geometry of oscillating bluff bodies. *J. Fluid Mech.* **208**, 375–393.

NAKAMURA, Y. & NAKASHIMA, M. 1986 Vortex excitation of prisms with elongated rectangular, H and ⊢ cross-sections. *J. Fluid Mech.* **163**, 149–169.

OKAJIMA, A., MIZOTA, T. & TANIDA, Y. 1983 Observation of flows around rectangular cylinders. *Proc. 3rd Intl Symp. on Flow Visualization, Michigan, University of Michigan*, pp. 193–199.

PARKER, R. & WELSH, M. C. 1983 Effects of sound on flow separation from blunt flat plates. *Intl J. Heat and Fluid Flow* **4**, 113–127.

ROCKWELL, D. & NAUDASCHER, E. 1978 Review-Self-sustaining of flow past cavities. *Trans. ASME* I: *J. Fluids Engng* **100**, 152–165.

STOKES, A. N. & WELSH, M. C. 1986 Flow-resonant sound interaction in a duct containing a plate, II: Square leading edge. *J. Sound Vib.* **104**, 55–73.

TANEDA, S. 1981 Amplification of artificial disturbances in turbulent boundary layers. *J. Phys. Soc. Japan* **50**, 2447–2449.

TANEDA, S. 1983 The main structure of turbulent boundary layers. *J. Phys. Soc. Japan* **52**, 4138–4144.

TOMONARI, Y. 1988 Aeroelastic galloping of a square-section cylinder in the Reynolds number range from 10^3 to 10^4. *Trans. Japan Soc. Aero. Space Sci.* **30**, 234–242.